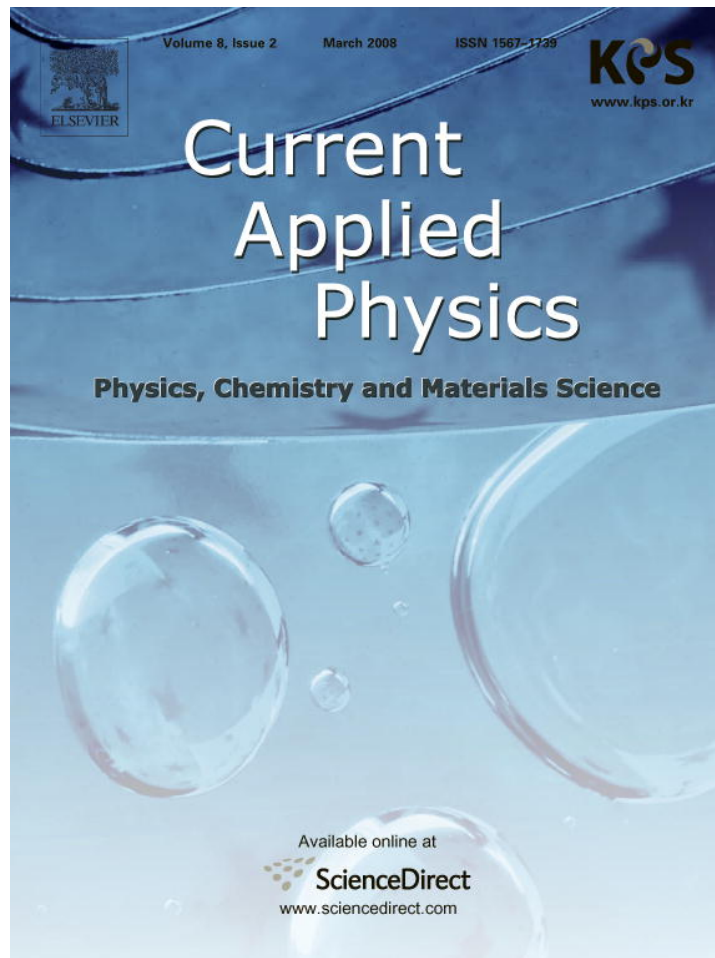


Provided for non-commercial research and education use.
Not for reproduction, distribution or commercial use.



This article was published in an Elsevier journal. The attached copy is furnished to the author for non-commercial research and education use, including for instruction at the author's institution, sharing with colleagues and providing to institution administration.

Other uses, including reproduction and distribution, or selling or licensing copies, or posting to personal, institutional or third party websites are prohibited.

In most cases authors are permitted to post their version of the article (e.g. in Word or Tex form) to their personal website or institutional repository. Authors requiring further information regarding Elsevier's archiving and manuscript policies are encouraged to visit:

<http://www.elsevier.com/copyright>



Growth, structure and physical properties of single crystals of pure and Pb-doped Bi-based high T_c superconductors [☆]

E. Giannini ^{a,*}, R. Gladyshevskii ^{a,b}, N. Clayton ^a, N. Musolino ^a, V. Garnier ^{a,1},
A. Piriou ^a, R. Flükiger ^a

^a Department of Physics of Condensed Matter (DPMC), University of Geneva, 24 quai Ernest-Ansermet, CH-1211 Geneva 4, Switzerland

^b Department of Inorganic Chemistry, Ivan Franko National University of L'viv Kyryla i Metodiya str. 6, UA-79005 L'viv, Ukraine

Received 8 July 2004; accepted 10 April 2007

Available online 16 June 2007

Abstract

Single crystals of $(\text{Bi}_{1-x}\text{Pb}_x)_2\text{Sr}_2\text{Ca}_2\text{Cu}_3\text{O}_{10+\delta}$ ($x = 0$ and 0.16) (sizes up to $3 \times 2 \times 0.1 \text{ mm}^3$) have been grown by means of a newly developed “vapour-assisted travelling solvent floating zone” technique (VA-TSFZ). Post-annealing under high pressure of O_2 (up to 10 MPa at $T = 500 \text{ }^\circ\text{C}$) was applied to enhance T_c (up to 111 K) and improve the homogeneity of the crystals ($\Delta T_c \leq 1 \text{ K}$). The structure of both Pb-free and Pb-doped Bi-2223 was refined for the first time from single crystal X-ray diffraction (XRD) data. The unit cell of the average structure is pseudo-tetragonal with $a = 5.4210(7)$, $b = 5.4133(6)$ and $c = 37.010(7) \text{ \AA}$, and $a = 5.395(1)$, $b = 5.413(1)$ and $c = 37.042(11) \text{ \AA}$, for the Pb-free and the Pb-doped phase, respectively. An incommensurate modulation in the direction of one of the short cell vectors has been defined ($\mathbf{q} \sim 0.21 \mathbf{a}^*$), however, the structure can be conveniently described in a supercell with a fivefold volume ($a = 27.105(4) \text{ \AA}$). With respect to the “non-modulated” structure, one additional oxygen atom for ten initial O was found to be inserted into the BiO layers. The superconducting anisotropy of Bi-2223 was found to be ~ 50 , from measurements of the lower critical field. The anisotropy of Bi-2223 is significantly reduced compared to that of Bi-2212, and this accounts for the enhanced irreversibility fields in Bi-2223. Furthermore, Bi-2223 has a higher critical current density, and a reduced magnetic relaxation rate compared to Bi-2212, which are both signatures of more effective pinning in Bi-2223 due to its reduced anisotropy.

© 2007 Elsevier B.V. All rights reserved.

PACS: 61.10.Nz; 74.25.Ha; 74.72.Hs; 81.10.Fq

Keywords: Bi-2223; Crystals; Structure; Superconductors

1. Introduction

Only the $n = 1$ and $n = 2$ members of the $\text{Bi}_2\text{Sr}_2\text{Ca}_{n-1}\text{Cu}_n\text{O}_{4+2n+\delta}$ family of high T_c superconductors have been available so far as sizeable single crystals and extensively studied [1,2]. Fundamentals investigations on the $n = 3$ compound $\text{Bi}_2\text{Sr}_2\text{Ca}_2\text{Cu}_3\text{O}_{10}$ (from now on called Bi-2223) have been strongly hindered due to the lack of high quality single crystals and thin films. In spite of this,

the Pb-doped (Bi,Pb)-2223 compound is at present the most promising material for large scale applications of superconductivity at liquid N_2 temperature, and has been the subject of a tremendous research effort for more than 15 years. Few Bi-2223 crystals have been successfully grown in the recent past by the alkali-chloride flux [3–6] and by the travelling solvent floating zone method [7,8]. Large (up to $4 \times 2 \times 0.01 \text{ mm}^3$) Pb-free Bi-2223 crystals have been grown, but quite broad superconducting transitions are reported [7,8] and the structure of either the Pb-free or the Pb-doped has not been refined yet. In this paper, we report first the growth of large (sizes up to $2 \times 3 \times 0.1 \text{ mm}^3$), pure single crystals of both Bi-2223 and (Bi,Pb)-2223 using the newly developed VA-TSFZ

[☆] This paper was submitted for the proceedings of the MSU-HTSC VII.

* Corresponding author. Tel.: +41 22 379 60 76; fax: +41 22 379 68 69.
E-mail address: Enrico.Giannini@physics.unige.ch (E. Giannini).

¹ Present address: INSA – GEMPPM, 69621 Villeurbanne, France.

technique [9], which is a suitable technique for growing crystals in the presence of volatile elements such as Pb.

Thanks to the availability of high quality Bi-2223 and (Bi,Pb)-2223 crystals, we were able to refine the crystal structure of both phases from single crystal X-ray diffraction data. Results of the structure refinement are reported and discussed in this paper. The average structures can be in an orthorhombic space group $A2aa$, the cell parameters of the average subcells being $a = 5.4210(7) \text{ \AA}$, $b = 5.4133(6) \text{ \AA}$ and $c = 37.010(7) \text{ \AA}$ for the Pb-free phase and $a = 5.395(1) \text{ \AA}$, $b = 5.413(1) \text{ \AA}$ and $c = 37.042(11) \text{ \AA}$ for the Pb-doped phase. An incommensurate modulation in the direction of one of the short cell vectors has been defined ($\mathbf{q} \sim 0.21\mathbf{a}^*$). The superstructure was refined in an orthorhombic space group $P222$ using a fivefold commensurate supercell. A partial substitution of Bi for Ca was found in both phases.

The magnetic properties of the Bi-2223 crystals are reported in the last part of this paper. We have measured the superconducting anisotropy of Bi-2223, which is found to be substantially reduced compared to that of Bi-2212. As a consequence, pinning is more effective in Bi-2223 and the critical current densities and irreversibility fields are increased, compared to Bi-2212. The vortex phase diagram of Bi-2223 is drawn up to $\mu_0 H = 5 \text{ T}$.

2. Growth of Bi-2223 and (Bi,Pb)-2223 crystals

Pb-free and Pb-doped Bi-2223 crystals have been grown by using the newly developed vapour-assisted travelling solvent floating zone method (VA-TSFZ) [9]. For the Pb-free sample preparation, a home made precursor with a nominal cation ratio Bi:Sr:Ca:Cu = 2.1:1.9:2.0:3.0 was prepared starting from high purity oxides and carbonates. For the Pb-doped sample preparation, a commercial precursor rod (from NEXANS) was used, having a starting cation ratio Bi:Pb:Sr:Ca:Cu = 1.84:0.32:1.84:1.97:3.00. Zone melting was performed in a homemade image furnace equipped with two 400 W halogen lamps. The sample (both the feed and the seed rods) was held inside a vertical quartz chamber in which either vacuum or controlled atmosphere can be set (Fig. 1). In order to compensate for the Pb-losses occurring at high temperature, an internal source of Pb was added. By placing a ring crucible containing PbO close to the molten zone (shown in Fig. 1), at the temperature suited for sublimation of PbO, a Pb flux was created at the rate needed for compensating Pb-losses from the molten zone, thus allowing the growth of Pb-doped crystals. After a first fast zone melting, which increases the density of the precursor rods, a very slow zone melting stage was performed at a travelling velocity of 50–60 $\mu\text{m/h}$. Crystal growth was performed under a flowing 7%O₂–93%Ar atmosphere, both for Pb-free and Pb-doped samples. Details of the growth method are reported in [9]. In order to increase the transition temperature and homogenize the oxygen content, as-grown crystals were annealed under $p(\text{O}_2) = 0.1\text{--}40 \text{ MPa}$ at $T = 500 \text{ }^\circ\text{C}$ for 20–300 h. After annealing in oxygen, T_c up to 111 K and

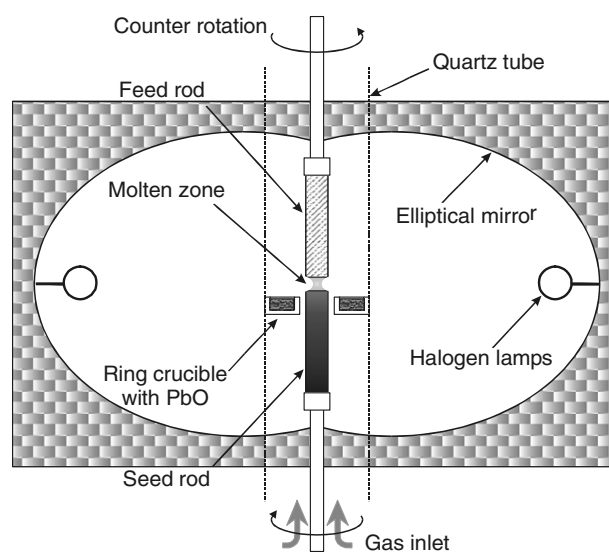


Fig. 1. Vertical cross section of the image furnace. During the crystal growth, both the feed and the seed rods move downwards and counter-rotate. The position of the crucible containing the internal source of PbO is shown.

transition widths as narrow as $\Delta T_c = 1 \text{ K}$ were obtained [9]. Morphology and chemical composition of the crystals were studied by SEM/EDX analysis performed in a Cambridge 438VP microscope coupled to a X-ray detector Noran Pioneer. The VA-TSFZ technique has proved to be successful in doping the Bi-2223 with Pb, and the average cation ratio was found to be Bi:Pb:Sr:Ca:Cu = 2.16:0.26:2.08:1.95:2.55 by EDX analysis.

3. Crystal structure of Bi-2223 and (Bi,Pb)-2223

The ideal structure of the Bi-2223 superconducting cuprate is constituted by oxygen deficient perovskite-like $\text{Sr}_2\text{Ca}_2\text{Cu}_3\text{O}_8$ blocks intercalated by rocksalt-like BiO bi-layers, forming a square-mesh layered sequence BiO–SrO–CuO₂–Ca–CuO₂–Ca–CuO₂–SrO–BiO. In all the members of the Bi-based family, extra oxygen atoms can be incorporated in the BiO layers, thus displacing the Bi atoms with respect to the perovskite-like blocks. (see [10] and references therein). This leads to the characteristic modulation with a modulation vector $\mathbf{q} = \lambda_1\mathbf{a}^* + \lambda_2\mathbf{c}^*$ [11]. No superstructure refinement has been performed so far on the Bi-2223 phase, and only the average subcell was refined from X-ray powder diffraction [12] and neutron powder diffraction [13,14].

We performed single crystals XRD at room temperature in a Stoe IPDS II diffractometer using a Mo $K\alpha$ radiation and a graphite monochromator. Fragments of crystals with sizes $0.18 \times 0.18 \times 0.01 \text{ mm}^3$ (Pb-free) and $0.25 \times 0.25 \times 0.02 \text{ mm}^3$ (Pb-doped) were used. Absorption correction was taken into account according to the size and the shape of the samples. Structure refinement was carried out by the least-squares method based on $|F|$ values using the *Xtal3.7* System [15]. Details of XRD data acquisition and structure

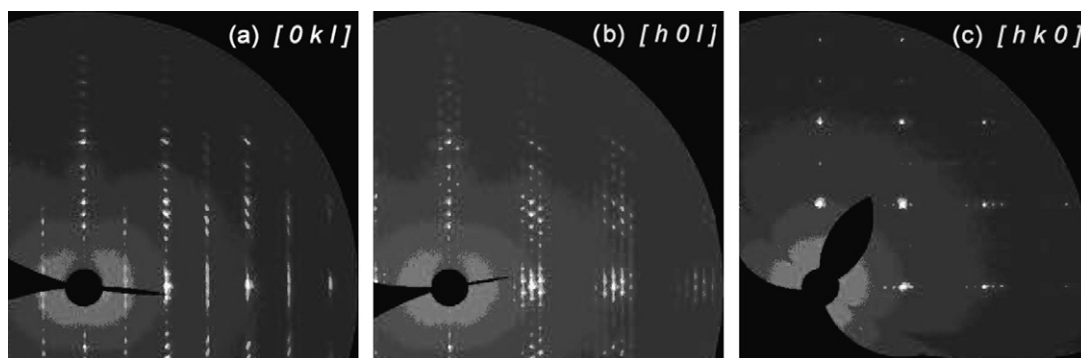


Fig. 2. X-ray diffraction patterns, taken with an Image Plate, of a Bi-2223 single crystal. Satellites due to the structure modulation are visible along $[0kl]$ and $[h0l]$.

refinement will be published elsewhere [16]. Diffraction patterns of the Pb-free Bi-2223 crystals are shown in Fig. 2. The presence of satellite reflections confirms the modulated structure and a modulation vector $\mathbf{q} \sim 0.21\mathbf{a}^*$ can be defined. The average structures of both the Pb-free and Pb-doped structures is orthorhombic and were refined in a noncentrosymmetric space group $A2aa$. The average structure was refined to $wR = 0.054$ and 0.070 for the Pb-free and Pb-doped phase, respectively ($wR = 1/\sigma^2(|F|_{\text{rel}})$). The cell parameters are listed in Table 1. In the Pb-doped structure, the orthorhombic distortion is enhanced and the c -axis is found to be slightly larger, as found in Pb-doped Bi-2212 [17]. The structure can be conveniently described in a orthorhombic supercell with fivefold volume ($a = 27.105(4)$ Å), and refined in the space group $P222$ (#16 in the International Tables for Crystallography). This representation makes it possible to locate and quantify extra oxygen atoms in the BiO layers. With respect to the “non-modulated” structure, additional oxygen atoms (one O atom per translation unit of the modulation wave, i.e. one extra O for ten initial O) were found to be inserted into the BiO layers, so that regions with a distorted rocksalt-type atom arrangement and regions with chains of corner-linked BiO_3 ψ -tetrahedra are formed. The average subcell is shown in Fig. 3a. The projections along the b axis of the supercell is shown in Fig. 3b. A detail of the BiO distorted layer is shown in Fig. 4, projected along the c axis. Approximately 8% of Bi

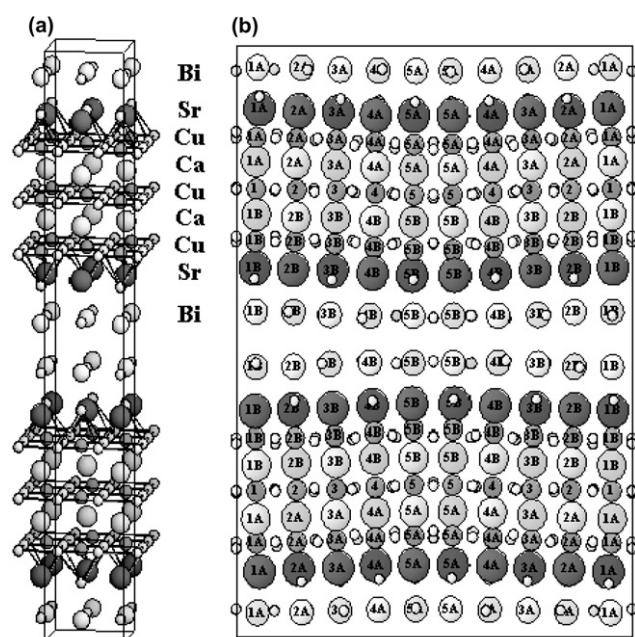


Fig. 3. (a) Average structure of the Bi-2223 phase. (b) Projection along b of the orthorhombic supercell. Modulated displacement along the c -axis is visible. Labels on atoms indicate independent atomic positions.

substitution was found on the Ca site, the refined composition being $\text{Bi}_{2.16}\text{Sr}_2\text{Ca}_{1.84}\text{Cu}_3\text{O}_{10.16}$. In the Pb-doped phase, the Bi/Ca substitution was found to be slightly

Table 1
Parameters of the structure refinement of both the Pb-free and Pb-doped Bi-2223

Space group	$\text{Bi}_{2.16}\text{Sr}_2\text{Ca}_{1.87}\text{Cu}_3\text{O}_{10.16}$		$(\text{Bi,Pb})_{2.12}\text{Sr}_2\text{Ca}_{1.94}\text{Cu}_3\text{O}_{10.13}$	
	Subcell	Supercell	Subcell	Supercell
	$A2aa$	$P222$	$A2aa$	$P222$
Cell parameters (Å)	$a = 5.4210(7)$ $b = 5.4133(6)$ $c = 37.009(7)$ $\mathbf{q} \sim 0.21\mathbf{a}^*$	$a = 27.105(4)$ $b = 5.4133(6)$ $c = 37.009(7)$	$a = 5.395(1)$ $b = 5.413(1)$ $c = 37.042(11)$ $\mathbf{q} \sim 0.20\mathbf{a}^*$	$a = 26.976(7)$ $b = 5.413(1)$ $c = 37.04(1)$
Atoms in the cell	76	384	76	384
Collected reflections	3801	40533	3728	39790
Unique reflections	656	6744	649	6668
Refined parameters	58	622	58	622
wR	0.054	0.096	0.070	0.097

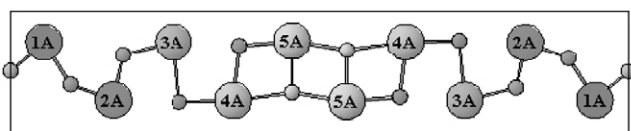


Fig. 4. Projection of BiO layers along [001]. The drawing shows the displacement of Bi and O atoms from the ideal rocksalt positions.

lower, approximately 5%, the refined composition being $(\text{Bi,Pb})_{2.12}\text{Sr}_2\text{Ca}_{1.87}\text{Cu}_3\text{O}_{10.13}$. The superstructure was refined to $wR = 0.096$ and 0.097 for the Pb-free and Pb-doped phase, respectively.

4. Superconducting properties of Bi-2223 crystals

The superconducting transition obtained by magnetic measurements (performed in a commercial SQUID magnetometer – Quantum Design) is shown in Fig. 5 for an optimally doped Bi-2223 crystal. The transition width as narrow as 1 K indicates the high quality of the crystal. The lower critical field (H_{c1}) was measured with the magnetic field applied parallel to the c -axis and then parallel to the ab -planes, and a measure of the superconducting anisotropy was obtained. These measurements were performed at very slow sweeping rate of the magnetic field, $dH/dt < 1 \times 10^{-4}$ Oe/s at low temperatures, in order not to be affected by surface barrier and geometrical effects [18]. The anisotropy of Bi-2223 was found to be $\gamma = H_{c1}(H//c)/H_{c1}(H//ab) \approx 50$ at $T = 30$ K. This value is between that of extremely anisotropic Bi-2212 ($\gamma = 165$) and $\text{YBa}_2\text{Cu}_3\text{O}_7$ ($\gamma = 5$ – 7). We have measured the lower critical field down to $T = 10$ K and have found the value $H_{c1}(10 \text{ K}) \sim 530$ Oe. H_{c1} was extrapolated down to $T = 0$ K and the in-plane penetration depth, λ_{ab} was obtained at $T = 0$ K using the expression $H_{c1} = (\Phi_0/4\pi\lambda_{ab}^2) \ln\kappa$, $\lambda_{ab}(0) = 1200$ Å (where κ is the Ginzburg–Landau parameter, assumed to be $\kappa = 120$). Our choice of κ implies that the coherence length is $\xi = 10$ Å. For compar-

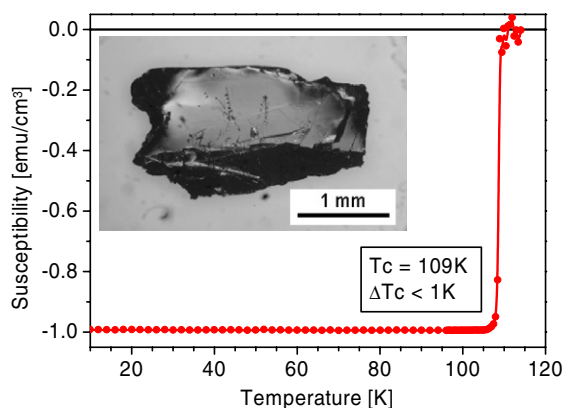


Fig. 5. Superconducting transition of an optimally doped Bi-2223 crystal at $T_c = 109$ K ($\Delta T_c \leq 1$ K). A picture of the crystal is shown in the inset.

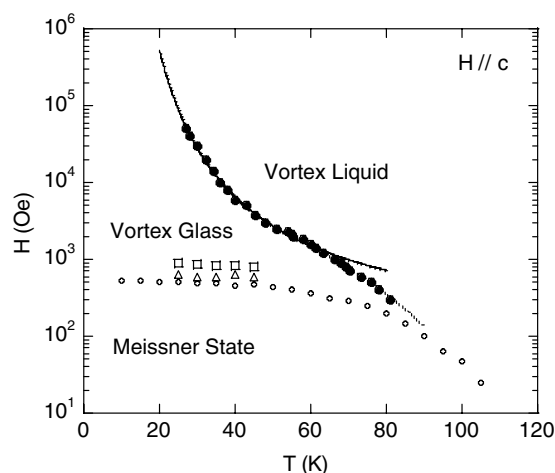


Fig. 6. Vortex phase diagram of Bi-2223 with $H//c$. Open circles are $H_{c1}(T)$, triangles and squares are the onset and the peak of the second peak. Filled circles indicate the irreversibility line.

ison, the penetration depth in $\text{Yba}_2\text{Cu}_3\text{O}_{7-\delta}$ is $\lambda_{ab}(0) = 1350$ Å and in Bi-2212, $\lambda_{ab}(0) = 3000$ Å.

The vortex phase diagram of Bi-2223 has been investigated and reported in [19] and is drawn in Fig. 6. The irreversibility line (IL) was measured by acquiring field-cooled (FC) and zero-field-cooled (ZFC) magnetisation data using a SQUID magnetometer. The irreversibility temperature was identified by a “kink” above the merging of the FC and ZFC data, as discussed in [19]. When plotted together with the IL of Bi-2212 as a function of reduced temperature T/T_c , the irreversibility line of Bi-2223 is found to be translated to higher magnetic fields compared to that of Bi-2212. We believe that the observed positions of the IL are due to the different values of the anisotropy we have measured for Bi-2223 ($\gamma = 50$) and Bi-2212 ($\gamma = 165$). Magnetic measurements on our single crystals revealed the emergence of a second peak (SP) in the $m(H)$ hysteresis loops over a limited temperature range ($T = 30$ – 50 K), as also observed in Bi-2212 and YBCO. The onset and the peak of the SP are plotted in the H vs T phase diagram (Fig. 6) and mark the transition of the vortex lattice from the well ordered Bragg-Glass phase toward a highly disordered phase. The high value of the position of the SP in Bi-2223, $H_{2nd} \approx 600$ Oe, compared to optimally doped Bi-2212, confirms the larger elasticity of the vortex lattice in Bi-2223, which is a consequence of its reduced anisotropy compared to that of Bi-2212. For a given reduced temperature, the J_c values of the Bi-2223 crystal are always higher than those of the Bi-2212 crystal, showing that pinning is intrinsically more efficient in Bi-2223 than in Bi-2212 crystals.

5. Conclusions

We have grown large and high quality single crystals of both Pb-free and Pb-doped Bi-2223 which display sharp

superconducting transitions. The structure of these phases was refined for the first time from single crystal X-ray diffraction data. The unit cell of the average structure is pseudo-tetragonal with $a = 5.4210(7)$, $b = 5.4133(6)$ and $c = 37.010(7)$ Å, and $a = 5.395(1)$, $b = 5.413(1)$ and $c = 37.042(11)$ Å, for the Pb-free and the Pb-doped phase, respectively, and an incommensurate modulation $q \sim 0.21 a^*$ has been defined. However, the structure can be conveniently described in a supercell with a fivefold volume ($a = 27.105(4)$ Å) and refined in the space group $P222$. Additional oxygen atoms were found to be incorporated in the BiO layers, and Bi was found to partially (5–8%) substitute for Ca.

The superconducting properties of Bi-2223 have been investigated through measurements of the lower critical field. Bi-2223 is found to have an anisotropy of $\gamma = 50$, which is substantially reduced from that of Bi-2212 ($\gamma = 165$). The irreversibility line of Bi-2223 has been measured, and is translated to higher magnetic fields compared to Bi-2212, which is mainly due to the reduced anisotropy of Bi-2223.

Acknowledgements

Authors gratefully acknowledge Dr. Radovan Černý of the Department of Crystallography for assistance and fruitful discussions.

This work was supported by the Swiss National Research Fund and the Swiss NCCR on Materials with Novel Electronic Properties (MaNEP).

References

- [1] M. Matsumoto, J. Shirafuji, K. Kitahama, S. Kawai, I. Shigaki, Y. Kawate, Phys. C 185–189 (1991) 455.
- [2] T. Mochiku, Bismuth-based high-temperature superconductors, in: H. Maeda, K. Togano (Eds.), Dekker, New York, 1996, p. 227.
- [3] G. Balestrino, E. Milani, A. Paoletti, A. Tebano, Y.H. Wang, A. Ruosi, R. Vaglio, M. Valentino, P. Paroli, Appl. Phys. Lett. 64 (13) (1994) 1735.
- [4] S. Chu, M. McHenry, J. Mater. Res. 13 (3) (1998) 589.
- [5] J.I. Gorina, G.A. Kaljuzhnaia, V.P. Martovitsky, V.V. Rodin, N.N. Sentjurina, V.A. Stepanov, Solid State Commun. 110 (1999) 287.
- [6] S. Lee, S. Yamamoto, S. Tajima, Phys. C 357–360 (2001) 341.
- [7] T. Fujii, T. Watanabe, A. Matsuda, J. Cryst. Growth. 223 (2001) 175.
- [8] B. Liang, C.T. Lin, P. Shang, G. Yang, Phys. C 383 (2002) 75.
- [9] E. Giannini, V. Garnier, R. Gladyshevskii, R. Flükiger, Supercond. Sci. Technol. 17 (2004) 220.
- [10] R. Gladyshevskii, P. Galez, Crystal Structures of High- T_c Superconducting Cuprates, Handbook of Superconductivity, Academic Press, 2000, p. 267.
- [11] S. Ikeda, K. Aota, T. Hatano, K. Ogawa, Jpn. J. Appl. Phys. 27 (1988) L2040.
- [12] W. Carrillo-Cabrera, W. Göpel, Phys. C 161 (1989) 373.
- [13] G. Miehe, T. Vogt, H. Fuess, M. Wilhelm, Phys. C 171 (1990) 339.
- [14] E. Bellingeri, G. Grasso, R.E. Gladyshevskii, M. Dhallé, R. Flükiger, Phys. C 329 (2000) 267.
- [15] S.R. Hall, D.J. du Boulay, R. Olthof-Hazekamp (Eds.), *Xtal3.7* System, University of Western Australia, 2000.
- [16] R. Gladyshevskii, E. Giannini, R. Černý, R. Flükiger, in press.
- [17] R. Gladyshevskii, N. Musolino, Phys. Rev. B 70 (2004) 184522.
- [18] N. Clayton, N. Musolino, E. Giannini, V. Garnier, R. Flükiger, presented at ICMC 2004, 10th–13th February 2004, Wollongong, Australia.
- [19] N. Clayton, N. Musolino, E. Giannini, V. Garnier, R. Flükiger, Supercond. Sci. Technol. 17 (2004) S563.